

2D and 3D Back-analysis of a landslide in Egremnoi caused by the November 17 2015 Lefkada earthquake

Kallimogiannis, Vasileios¹, Saroglou, Charalampos
National Technical University of Athens, Greece

Zekkos, Dimitrios
University of Michigan, Ann Arbor, USA

Manousakis, John
Elxis Group, Athens, Greece

ABSTRACT

On November 17th 2015, a M_w 6.5 earthquake struck the island of Lefkada in Greece. The shaking caused landslides and rockfalls particularly in the western part of the island. The stability of a major landslide that occurred in Egremnoi beach, was investigated with the objective to back-calculate the shear strength of the failed ground, which is geologically characterized as a disintegrated and highly tectonized limestone. The geometry of the landslide was determined by comparing the surface of the ground before and after the earthquake. Pre- and post-earthquake surfaces were derived using the National cadastre surface model and imagery collected from an Unmanned Aerial Vehicle (UAV), respectively. Pseudo-static two-dimensional and three-dimensional slope stability analyses were performed. The seismic coefficient $k_{h,E}$ was determined using strong motion data recorded at Vasiliki and Chortata station located in the vicinity (<10 km) of the landslide. The back-calculated shear strength of the tectonized limestone is found to be similar to that of a hard soil – weak rock. The analysis provides a reliable estimate of rockmass shear strength since sampling and laboratory testing of the material is difficult.

Keywords: earthquake, landslide, Lefkada island, stability, tectonized breccia limestone, mylonite

INTRODUCTION

On November 17 2015 at 07:10:07 UTC a strong, shallow M_w 6.5 earthquake occurred on the island of Lefkada along a NNE–SSW striking dextral strike-slip seismic fault with a reverse component that dips east at a high angle of about $70 \pm 5^\circ$ (Lekkas et al., 2018). The seismotectonic setting is characterized primarily by the Hellenic subduction in the South that is connected to the Adriatic collision in the North through the right-lateral Cephalonia fault also called Cephalonia-Lefkada Transform fault – KLTF. KLTF consists of at least two segments: the northern (Lefkada segment), striking NNE-SSW, which is approximately 40 km long, and the southern (Cephalonia segment), striking NE-SW, and is 60 km long (Rondoyanni et al., 2012). The 2015 earthquake ruptured a coastal fault that remained unruptured by the two large sub-events of the M_w 6.2 Lefkada double in 2003 (Sokos et al., 2016). The epicenter is located on Lefkada island, according to the National Observatory of Athens, Institute of Geodynamics of Greece (www.gein.noa.gr).

¹ Corresponding Author: V. Kallimogiannis, *National Technical University of Athens, vkallim@hotmail.com*

The event caused structural damage and triggered rock falls, rock slides, landslides, road fill failures and small-size liquefaction features (Papathanasiou et al., 2017, Saroglou et al. 2018) especially in the western part of Lefkada. In the area of Egremnoi, the shaking caused landslides due to the relatively low strength of the tectonized limestone, and the steep and high slopes along the western coastline. In the present study, a major landslide is back-analyzed to derive the mechanical properties of the limestone rockmass. The landslide is shown in Fig. 1, shortly after the earthquake and the debris is observed to cover part of the failure surface. The height of the entire slope is 195 meters and its average inclination is 47° .



Figure 1. The major landslide triggered by the M_w 6.5 earthquake at the site of Egremnoi (*Photo by news.in.gr*)

GEOLOGICAL FEATURES

Geotectonics of Lefkada island

The island of Lefkada consists of a carbonate sequence of the Ionian zone, limestones of Paxos (Apulia) zone restricted in the SW peninsula of the island and few outcrops of Ionian flysch (turbidites) and Miocene marls-sandstones mainly in the northern part of the island (Rondoyanni-Tsiambaou, 1997). The Ionian zone is separated from the Paxos zone by a thrust fault striking in NW-SE direction (Karababa & Pomoris, 2011).

The Ionian islands, which include Lefkada island, are located in the central part of the Ionian Sea which is one of the most seismically active regions in the Mediterranean and experience frequent M_w 5–6.5 earthquakes, as well as less frequent larger (up to 7.5) earthquakes. On average, Lefkada experiences at least one damaging earthquake every 18 years (Papathanassiou et al., 2005). Seismicity is primarily associated with dextral strike-slip faulting along the Cephalonia Transform Fault comprising the distinctive Cephalonia and Lefkada faults (Papazachos et al., 2001, Louvari et al., 1999; Karakostas et al., 2004). The NE-SW to NNE-SSW trending neotectonic main faults are normal structures with a significant right-lateral component, while some minor faults trending NW-SE exhibit left-lateral character (Papathanasiou, 2013).

Geology of the study area

The ground conditions in the area of Egremnoi were evaluated during a field reconnaissance expedition. The formations characterizing the Egremnoi area are; a) Limestone breccia and tectonized limestone breccias; b) Marly limestone with fossils; and c) Mylonite. The upper-cretaceous bedrock limestone is evident sporadically in the surface of the ground. The limestones in the study area belong to the Paxos zone. Tectonic stresses, due to the presence of major faults striking parallel to the slopes in the western part of the island, have resulted in the formation of tectonic breccia and mylonite with poor mechanical properties.

Testing on limestone breccias from five different areas in Greece (Koukis et al., 2001) indicates that the uniaxial compressive strength ranges between 16 and 51 MPa with an average value of 32.2 MPa. Kahraman et al. (2015) investigated the strength properties of Misis fault breccias in Turkey and the correlation of primary wave velocity V_p , shear wave velocity V_s and density with Volumetric block proportion (VBP). The average strength of limestone breccias in that study was equal to 40.3 MPa. The strength of the limestone breccias in Egremnoi site is expected to be lower than the strength of breccias at these sites. Furthermore, the rockmass strength of the materials in which the landslides occurred, is significantly lower.

Rockmass characterization of the landslide area

The landslide consists of tectonized limestone breccias and mylonite. Distinguishing between them is difficult as the area is remote and steep and field investigation on the landslide backscarp could not be conducted. Quantifying the mechanical properties of these ground materials is challenging. Sampling is practically impossible since even triple-tube diamond coring extensively disturbs the tectonized rock-mass whereas available rockmass classification systems do not apply on such materials. Therefore, back-analysis is the only direct method to determine their mechanical properties. Although we recognize that mylonite is a weaker tectonized breccia without distinct structure, in the conducted back-analysis one uniform material was assumed to estimate the average shear strength of the ground.

METHODOLOGY

Introduction

Although many more landslides occurred during the M_w 6.5 earthquake (Zekkos et al. 2017), in this paper, one main landslide is presented. To derive the landslide's geometry, field mapping with Unmanned Aerial Vehicles (UAVs) and data from the National Cadastre were utilized. The Digital Elevation Models (DEMs) showed that the rupture surface is near-circular indicating that the main failure mechanism was shear failure. The landslide was back-analyzed using 2D and 3D limit equilibrium analyses and the software TSLOPE (TAGA Engineering Software Ltd, 2019).

Pre-earthquake geometry and field mapping of post-earthquake slopes

The Phantom 3 Pro UAV that is equipped with a 12 MP camera was used to collect overlapping imagery of the Egremnoi slopes. The region was mapped just two days after the earthquake and in April 2016. UAVs are nowadays valuable data acquisition platforms for inspection, surveillance and mapping purposes (Greenwood et al. 2019, Nex & Remondino, 2014). UAVs are valuable to derive topography for natural slopes that may be prone to geological hazards, such as landslides or rockfalls. In this study, the images were collected using 80% vertical and 60% lateral overlapping in order to produce a 3D Point Cloud model using the Structure-From-Motion (SfM) technique (Zekkos et al. 2018, Fonstad et al. 2013; Micheletti et al., 2015). The density of the 3D Point Clouds was 140 points per m^2 . These data provided the surface of the ground after the earthquake. It is pointed out that, in April 2016, the debris shown in Figure 1 was eroded by wave action and the failure surface was exposed.

The pre-earthquake geometry was determined via photogrammetric data from the Hellenic Cadastre spatial database. The digital elevation model (DEM) implemented, was created for the production of orthophotos from aerial photo strips captured between 2007 and 2009 and has a 5 m pixel size on the ground. The geometric accuracy of the product is $RMSE_z \leq 2.00$ m and absolute accuracy ≤ 3.92 m with a confidence level of 95%.

Evaluation of the seismic load that triggered the landslides

The seismic load that triggered the landslides was considered using the pseudo-static method (Terzaghi, 1950). The pseudo-static method simplistically uses a constant horizontal and vertical force on the slope by considering seismic coefficients $k_{h,E}$ and $k_{v,E}$, respectively. Usually, the instabilities are caused by the horizontal load and therefore, the vertical load can be neglected. The selection of $k_{h,E}$ is critical to evaluate the seismic stability of the slope. Two methodologies, the Eurocode 8 standard and the U.S. NCHRP 12-70 / FHWA (2011) guideline, were selected to derive $k_{h,E}$.

Eurocode EC-8 standard

The seismic coefficient $k_{h,E}$ acting on the ground mass according to Eurocode EC-8 standard is calculated as:

$$k_{hE} = 0.5 * S * S_T * PGA_{ground} \quad [1]$$

where S: Soil parameter, S_T : coefficient of topographic amplification, PGA: Peak ground acceleration.

Since, based on field observations, the ground can be characterized as type B and the slopes are higher than 30 meters with an inclination of more than 15° , the S coefficient was set to 1.20 and S_T coefficient must be greater than 1.40. Considering a numerical evaluation of topography amplification for similar type of slopes (Pagliaroli et al., 2007), a value of 1.50 is selected. PGA was determined by using data from two acceleration station that were both located at similar distance from the epicenter of the earthquake as the landslide being investigated (Vasiliki and Chortata). The PGA values in Vasiliki and Chortata stations were equal to 0.36g and 0.42g, respectively. Therefore, an average PGA equal to 0.39g was used. Chortata and Vasiliki stations are located about 10 km and 4.5 km from the Egremnoi site, respectively. Therefore, $k_{h,E}$ coefficient was calculated equal to 0.35g.

NCHRP 12-70/FHWA (2011)

The NCHRP 12-70/ FHWA (2011) recommendation determines the horizontal seismic acceleration coefficient as:

$$k_{hE} = a * F_{PGA} * PGA_{ground} \quad [2]$$

where a is a slope height factor, F_{PGA} is the AASHTO peak ground acceleration site factor, and PGA is the average peak ground acceleration set equal to 0.39g.

$$a = 1.2 * [1 + 0.01 * H * (0.5 * \beta - 1)] \quad [3]$$

$$\beta = \frac{F_v * S_1}{F_{PGA} * PGA} \quad [4]$$

where H is the height of the slope, F_v is the AASHTO site factor for the spectral acceleration at 1 second and S_1 is the spectral acceleration at 1 second for Site Class B.

According to the NCHRP recommendations, slope heights greater than 30 m do not further amplify the motion. Thus, a maximum height of 30 m is used. Coefficient S_1 was calculated using the accelerograph of Vasiliki station, the one closest to the site of interest. F_v and F_{PGA} were determined for soil type B, considering the S_1 and PGA, respectively. Based on these considerations, the values of the parameters are: $S_1=0.53g$; $F_v=1.00$; $F_{PGA}=1.00$; $\beta=1.36$; $\alpha=0.82$.

Thus, the $k_{h,E}$ coefficient using the NCHRP 12-70 / FHWA procedure is equal to 0.32g, which is similar to the 0.35g value from EC-8. A value of 0.35g was used in the stability analyses.

Back-analysis

2D and 3D limit equilibrium analyses were conducted using Spencer's limit equilibrium method (Spencer, 1967). The 3D method of columns, which is the equivalent of the method of slices in 3 dimensions, was utilized to back-analyze the landslide. The ground mass is divided into a number of vertical columns, each with an approximately square cross-section. TSLOPE (Tagasoft, 2019) was utilized for the analyses. The unit weight of the ground was assumed equal to 22 kN/m^3 , a typical value for a disintegrated limestone. The Mohr-Coulomb failure criterion was used to model the shear strength of the tectonized limestone.

RESULTS & DISCUSSION

Landslide characteristics

The geometric characteristics of the landslide were evaluated using the pre- and post- earthquake geometries. Volume calculation between pre-earthquake and post-earthquake models was accomplished using CloudCompare software with a procedure that relies on a rasterization process of each point cloud (2.5D grid surface). In this process, the 2.5D grid is computed, and the clouds are projected to deduce the volume as well as other statistics (surface area, matching cells, relative coverage of both clouds, etc.). Volume is computed by multiplying the elementary parallelepiped corresponding to the cell footprint by the difference in heights between the two 2.5D raster grids.

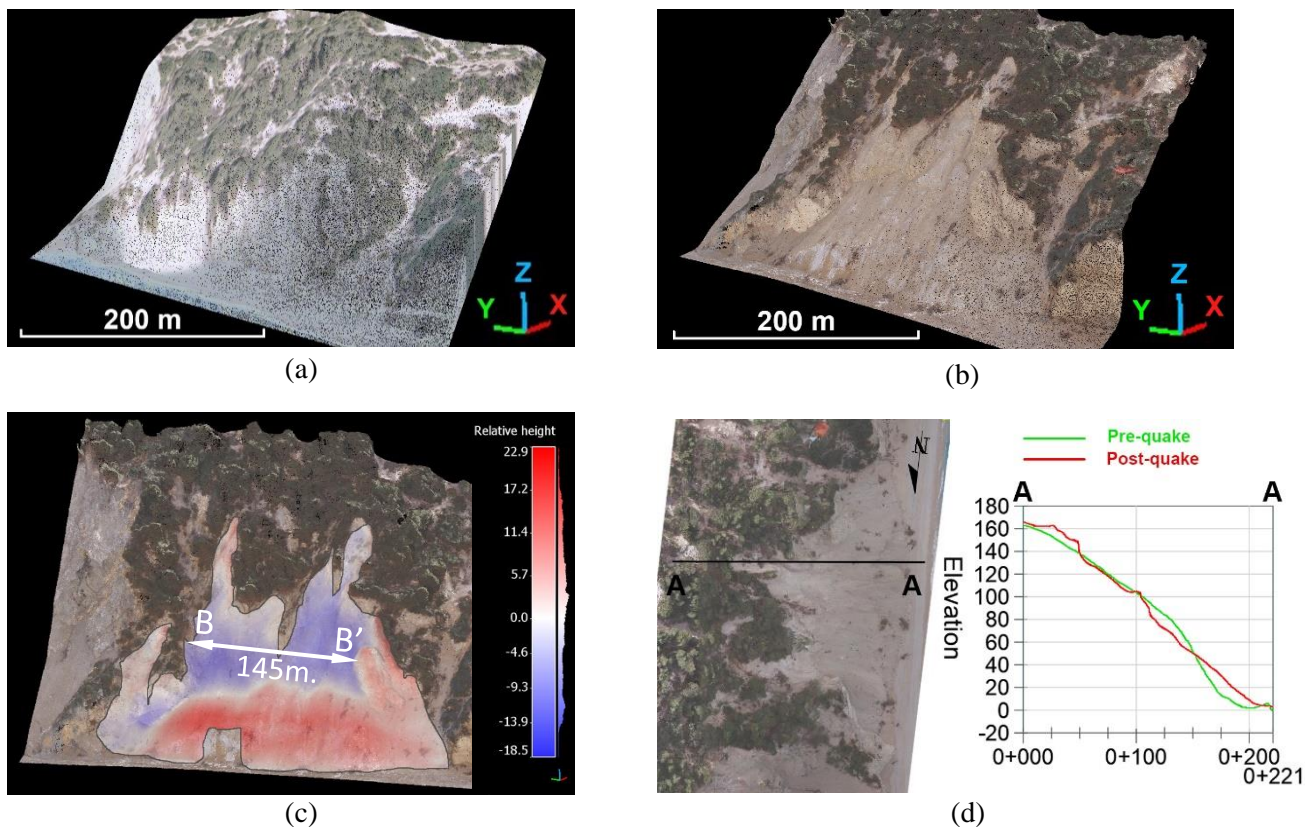


Figure 2. (a) Pre-earthquake (2009) 3D Point Cloud interpolated from 5 m Hellenic Cadastre DEM, (b) Post-earthquake (April 2017) 3D Point Cloud generated by SfM processing based on UAV survey, (c) Pre-post volume calculations presented as relative heights from reference surface (pre-quake DEM) with a 145-m section (BB') shown for scale; (d) Longitudinal cross-section (AA') through landslide showing pre-earthquake and post-earthquake geometry (in m).

Fig. 2 illustrates the before and after the earthquake surfaces as well as the volume loss and gain using a scale colored to illustrate height differences between the two 2.5D surfaces. A 2D longitudinal cross-section through the landslide is also shown in Fig. 2d. A height loss of up to 18.5 m is observed near the landslide crest and a gain in height of 22.9 m due to deposition of the debris at the toe of the landslide is also measured. The volume loss due to landsliding is calculated equal to $61,299 \text{ m}^3$ while the debris volume at the toe of the slope was

calculated at about 113,323 m³. The average depth of the slope is 5.8 m, indicating relatively shallow sliding given the slope's height, which exceeds 200 m.

The failure surface is illustrated in TSLOPE and compared with the real geometry in Figure 3. During the UAV survey in April 2016, debris had been removed and the slip surface was revealed. The geometry of the landslide is complex. Its width remains relatively constant while its length (top-bottom distance) varies significantly. The modeled surface is practically identical to the actual one. The calculated volume of the modeled landslide using the 3D method of columns was 65,000 m³, which is similar and slightly greater (~6%) than the volume measured in CloudCompare (61,299 m³). This is due to discretization differences caused by the column number limitation (maximum 200 columns) and is not considered significant. Analyses were conducted for a number of 2D cross-sections in an effort to identify the most critical ones for the complex geometry of the landslide. Fig. 3(b,c) shows the location of three selected one, that had among the lowest factors of safety. The 2D surfaces of failure for all the cross-sections (AA', CC' and DD') are shown in Fig. 4.

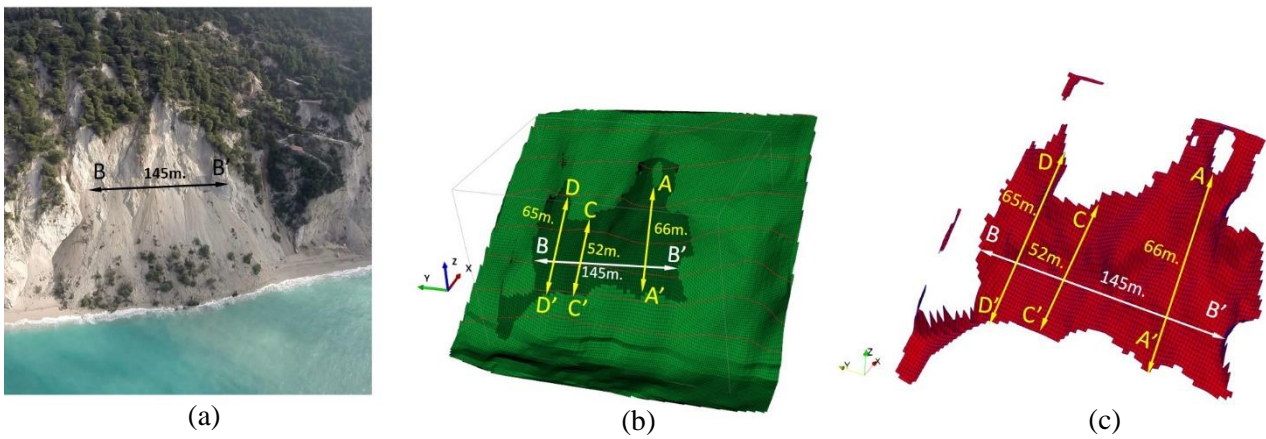


Figure 3. Comparison of failure geometry from (a) photographic data after the earthquake; (b) 3D method of columns illustration in TSLOPE measured both in TSLOPE; and (c) The failure surface projected in TSLOPE. A 145-m. BB' length measured both in TSLOPE and CloudCompare along with the two cross-sections (AA', CC' and DD') used for the 2D analyses are also shown.

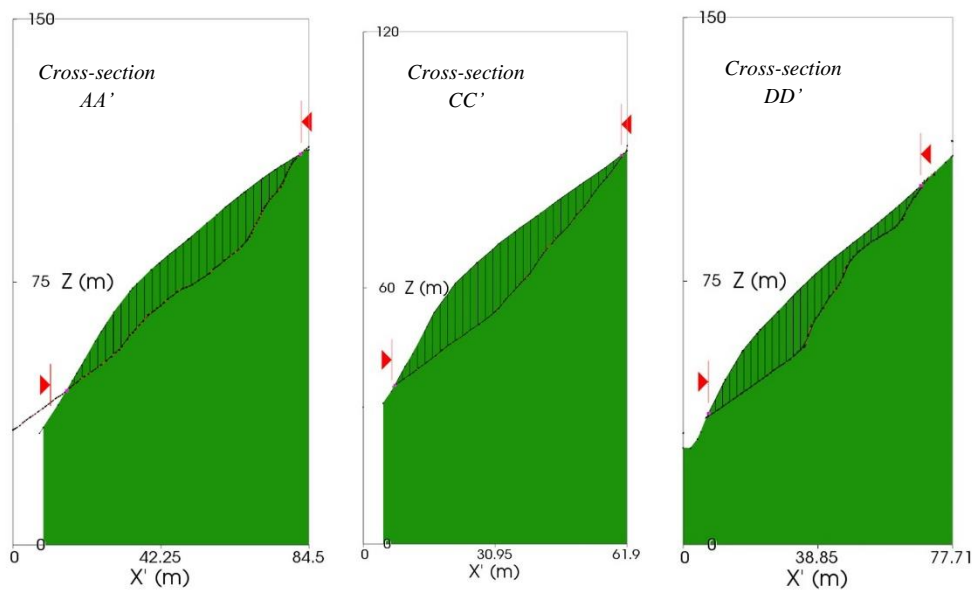


Figure 4. 2-D stability analyses along AA', CC' and DD' cross-sections.

Back analysis results

In back-calculating the shear strength of the material using the Mohr-Coulomb envelope, pairs of the two parameters, cohesion and friction angle, were derived since none of the two are known. Thus, the results are presented in terms of c - ϕ envelopes, and are shown in Fig. 5.

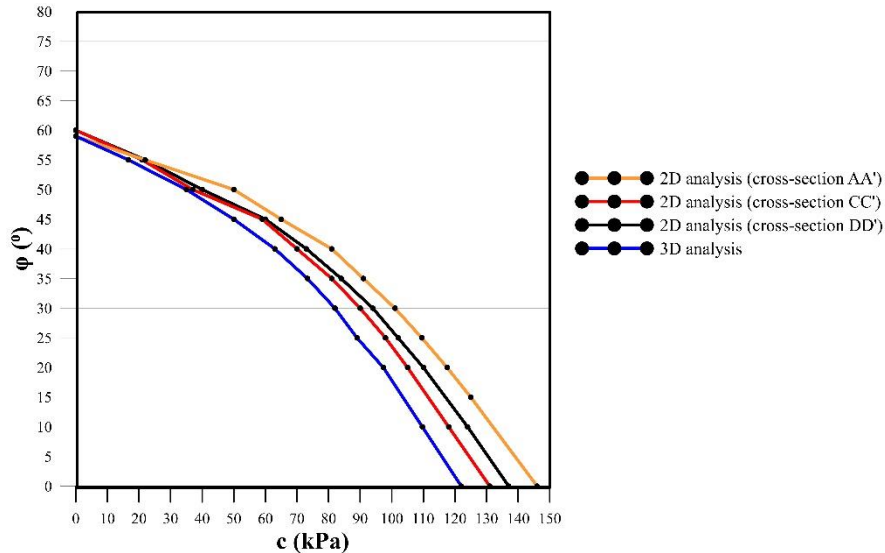


Figure 5. c - ϕ envelopes of 2D and 3D analyses for the landslide in Egremnoi site.

First, the strength parameters derived from the 2D analyses are higher than the strength parameters from 3D analysis, which is consistent with previous studies (Hovland, 1977; Duncan et al., 2014; Fomenko & Zerkal, 2011; Reyes & Parra, 2014; Ćorić et al., 2015) assuming that a critical cross-section is examined. However, Bromhead (2004) states that 3D analyses can sometimes produce lower safety factors compared to 2D analyses. Moreover, 2D analysis of cross section CC' is more conservative than 2D analysis of cross-section AA' and DD' showing that it is the most critical among all the cross-section examined.

2D stability analyses are plane strain, i.e., assume that the slope is infinitely long in the direction perpendicular to the plane of analysis while the failure is assumed to occur simultaneously along the entire length of the slope. A two-dimensional (plane strain) cross section is examined, and equilibrium is considered in just two directions. On the other hand, most slope failures are finite, and most failure surfaces are three dimensional, and often bowl-shaped (Duncan et al., 2014). Leshchinsky & Huang (1992) suggest that shear strength should not be back-calculated using 2D analyses for landslides with major 3D effects as this will result in overestimation of strength. 2D and 3D limit equilibrium safety factors usually differ up to 10% (Ćorić et al., 2012) but in some cases this difference may range from 15%-50% (Hadzi-Nikovic et al, 2013). In the present study, for cross-sections AA', CC' and DD' the 2D shear strength was found to be 15.4%, 6.8% and 9.5%, respectively, higher compared to that calculated in 3D.

Note that a factor of safety (FS) equal to 1 was assumed in the back-analysis. However, the actual value of the FS during the earthquake-induced failure may have been less than 1. Therefore, it is pointed out that the results derived from the back-analysis represent an upper limit of the material's shear strength.

Based on these results, the mechanical properties of the tectonized material are poor, as anticipated. Disintegration due to tectonic stresses reduced the material's strength to that of a hard soil/weak rock. According to geologic investigation conducted on the site by the authors, the friction angle of the tectonized limestone may range from 35° to 45° , limiting the possible cohesion-friction angle combinations. On average, a uniaxial compressive strength of 0.27 MPa was calculated.

The estimated strength is that of the material engaged in the landslide, which is near the surface of the ground. We hypothesized that at greater depths, the limestone will exhibit greater mechanical characteristics, limiting the landslide to shallower depths. To investigate this hypothesis, stability analyses using the derived strengths

were conducted to investigate deeper failure surfaces. Deeper landslides were also found to be unstable for the same assumed strength, but given the absence of such deeper landslides, higher strength parameters are expected at depth.

Impact of seismic coefficient $k_{h,E}$

Despite the existence of strong motion recordings in the vicinity of the site, there is still some uncertainty associated with deriving an equivalent seismic coefficient. To investigate the sensitivity of the results to such a variation of seismic coefficient, additional analyses were conducted for a range of $k_{h,E}$ values. The results of back-analysis for four different seismic coefficient values are presented in Fig. 6. Small changes from the assumed value of 0.35g would affect the results, but not drastically. Therefore, the utilization of the aforementioned methodologies for calculation of the $k_{h,E}$ value is adequate.

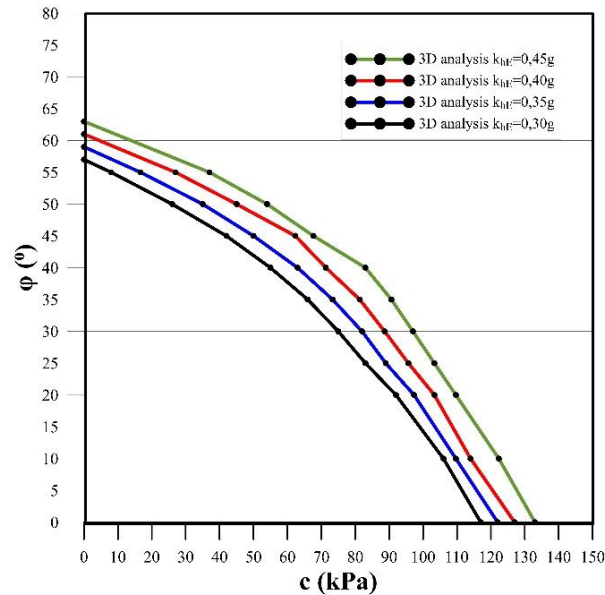


Figure 6. C- ϕ envelopes for 4 different seismic coefficient $k_{h,E}$.

CONCLUSIONS

The mechanical properties of a tectonized limestone that was engaged in a major ($>60,000 \text{ m}^3$) landslide in Egremnoi beach that failed during the 2015 Lefkada earthquake was investigated. The limestone is highly disintegrated due to intense tectonic activity forming either a tectonic limestone breccia that consists of irregular rock fragments or a mylonite. The landslide was back-analyzed using before and after 3D geometries. The back-calculated strengths, which represent upper limit estimates of the material's shear strength are low and resemble those of a weak rock / hard soil. Field observations indicate a range of friction angle from 35° to 45° with cohesions of 50-75 kPa. Combining the possible c- ϕ pairs, the average uniaxial compressive strength of the material is 0.27 MPa. Sensitivity analyses that were conducted to investigate the impact of $k_{h,E}$ showed that a minor variation of the seismic coefficient from the assumed value will not result in a significant change in strength parameters. Back-analysis, such as the one conducted in this study, is considered the most reliable method to derive mechanical properties of such geomaterials, as sampling and laboratory testing are extremely difficult while the application of common rock mass classification systems for strength characterization is not reliable.

ACKNOWLEDGEMENT

We acknowledge the support provided by Dr. Ian Brown and the team at TAGA Engineering Software Ltd, who provided us with the 3D limit equilibrium slope stability analysis package TSLOPE. Partial funding was

provided by USGS National Earthquake Hazards Reduction Program (NEHRP) grant G17AP00088. Any opinions, findings, conclusions, and recommendations expressed in this paper are those of the authors and do not necessarily reflect the views of the USGS.

REFERENCES

- Bromhead, E.N. (2004). Landslide slip surfaces: their origins, behaviour and geometry. Keynote paper. Proceedings, 9th International Symposium on Landslides, Rio de Janeiro. Balkema, Amsterdam, Vol. 1, 3–22.
- Ćorić, S., Ćaki, L., Rakić, D., Ubiparić, B., Berisavljević, Z. (2012). Geotechnical aspects of three dimensional stability analysis of landslides, 12 iNDiS 2012: Planning, design, construction and renewal in the civil engineering International Scientific Conference, NoviSad, November, 2012. pp. 361–368, ISBN 978-86-7892-453-8, COBISS.SR ID 275523335
- Ćorić, S., Rakić, D., Hadzi-Nikovic, G., Vladan, V. (2015). Three dimensional approach to stability analysis of landslide Mokra Gora. 2st Regional Symposium on Landslides in the Adriatic-Balkan Region - ReSyLAB 2015At: Belgrade, Serbia, 14th-16th May. pp. 62-65
- CloudCompare (version 2.6) [GPL software]. (2015). Retrieved from <http://www.cloudcompare.org/>
- Duncan, J., Stephen, G., Wright, Brandon, T.L. (2014). Soil strength and slope stability. Published by John Wiley & Sons, Inc., Hoboken, New Jersey. 2nd edition. ISBN 978-1-118-65165-0 (cloth); ISBN 978-1-118-91795-4 (ebk); ISBN 978-1-118-91796-1 (ebk).
- Eurocode 8, (2003). Design of structures for earthquake resistance, Part 5: Foundations, retaining structures and geotechnical aspects, CEN-ENV, European Committee for Standardization, Brussels.
- Fomenko, I.K. and Zerkal, V. (2011). Three-dimensional slope stability analysis. Proceedings of the Technical Meeting TC207: Workshop on Soil-Structure Interaction and Retaining Walls, p. 169-172.
- Fonstad, M.A., Dietrich, J.T., Courville, B.C., Carbonneau, P.E. (2013). Topographic structure from motion: a new development in photogrammetric measurements. *Earth Surface Processes and Landforms* 20: 817-827.
- Greenwood, W., Lynch, J.P., Zekkos, D. (2019). Applications of UAVs in Civil Infrastructure. *Journal of Infrastructure Systems*. 25. 10.1061/(ASCE)IS.1943-555X.0000464.
- Hovland, H.J. (1977). Three-dimensional slope stability analysis method. *ASCE J Geotech Eng Div.* 103. 971-986.
- Kahraman S., Alber M., Fener M., Gunaydin O. (2015). An assessment on the indirect determination of the volumetric block proportion of Misis fault breccia (Adana, Turkey). *Bull Eng Geol Environ* (2015) 74:899–907 DOI 10.1007/s10064-014-0666-9
- Karababa, F. and Pomonis, A. (2011) Damage data analysis and vulnerability estimation following the August 14, 2003 Lefkada Island, Greece. *Earthq Bull Earthq Eng* 9:1015–1046
- Karakostas, V., Papadimitriou, E., Papazachos, C. (2004). Properties of the 2003 Lefkada, Ionian Islands, Greece, Earthquake Seismic Sequence and Seismicity Triggering. *Bulletin of the Seismological Society of America*. 94. 1976-1981. 10.1785/012003254.
- Koukis G., Sabatakakis N., Tsiambaos G., Bourounis C. (2001). Correlations of physical and mechanical properties of rocks in Greece. *Bulleting of Geological Society of Greece*, vol. XXXIV/5, 1689-1695.
- Lekkas, E., Mavroulis, S., Carydis, P., Alexoudi, V. (2018). The 17 November 2015 Mw 6.4 Lefkas (Ionian Sea, Western Greece) Earthquake: Impact on Environment and Buildings. *Geotechnical and Geological Engineering*. 36. 10.1007/s10706-018-0452-8.
- Leshchinsky, D. and Huang, C. C. (1992). Generalized three-dimensional slope-stability analysis, *Journal of Geotechnical Engineering*, 18(11), 1748–1764.

- Louvari, E., Kiratzi A.A., Papazachos B.C. (1999). The Cephalonia Transform Fault and its extension to western Lefkada Island (Greece). *Tectonophysics* 308, 223–236.
- Micheletti, N., Chandler, J.H., Lane, S.N. (2015). Structure from motion (SFM) photogrammetry. IN: Clarke, L.E. and Nield, J.M. (Eds.) *Geomorphological Techniques (Online Edition)*. London: British Society for Geomorphology. ISSN: 2047-0371, Chap. 2, Sec. 2.2
- Nex, F. and Remondino, F. (2014). UAV for 3D mapping applications: A review. *Applied Geomatics*. 6. 10.1007/s12518-013-0120-x.
- Pagliaroli, A., Lanzo, G., D’Elia, B., Costanzo, A., Silvestri, F. (2007). Topographic amplification factors associated to cliff morphology: numerical results from two case studies in Southern Italy and comparison with EC8 recommendations. In *Proceedings of the Workshop on Geotechnical Aspects of EC8, 14th European Conference on Soil Mechanics and Geotechnical Engineering Madrid, Spain, 25 September 2007*. Edited by M. Mau-geri. Millpress Science Publishers, Rotterdam, the Netherlands. Chap. 8.
- Papathanassiou, G., Pavlides, S., & Ganas, A. (2005). The 2003 Lefkada earthquake: Field observations and preliminary microzonation map based on liquefaction potential index for the town of Lefkada. *Engineering Geology*, 82(1), 12–31. doi:10.1016/j.enggeo.2005.08.006.
- Papathanassiou, G., Valkaniotis, S., Ganas, A., Pavlides, S. (2013). GIS-based statistical analysis of the spatial distribution of earthquake-induced landslides in the island of Lefkada, Ionian Islands, Greece. *Landslides* 10 (6):771–783. <http://dx.doi.org/10.1007/s10346-012-0357S>.
- Papathanassiou, G., Valkaniotis, S., Ganas, A., Grendas, N., and Kollia, E. (2017). The November 17th, 2015 Lefkada (Greece) strike-slip earthquake: Field mapping of generated failures and assessment of macroseismic intensity ESI-07. *Engineering Geology*, 220 (July 2016), 13–30. <https://doi.org/10.1016/j.enggeo.2017.010.19>
- Papazachos, B.C., Mountrakis, D.M., Papazachos, C.B., Tranos, M.D., Karakaisis, G.F., Savvaidis A.S. (2001). The faults that caused the known strong earthquakes in Greece and surrounding areas during 5th century B.C. up to present, in *Proc. 2nd Conf. Earthquake Eng. and Eng. Seism.*, 2–30 September 2001, Thessaloniki, Greece, 1, 17–26
- Reyes, A. and Parra, D. (2014). 3-D slope stability analysis by the limit equilibrium method of a mine waste dump, *Proceedings of the 18th International Conference on Tailings and Mine Waste, Keystone, Colorado: Colorado State University*: pp. 257–271.
- Rondoyanni-Tsiambaou, Th. (1997). Les seismes et l’environnement geologique de l’île de Lefkade, Grece: Passe et Futur. In: Marinos, et al., (Eds.), *Engineering Geology and the Environment*. Balkema, 1469– 1474
- Rondoyanni, Th., Sakellariou, M., Baskoutas, J., Christodoulou, N. (2012). Evaluation of active faulting and earthquake secondary effects in Lefkada Island, Ionian Sea, Greece: an overview. *Nat Hazards* 61:843. <https://doi.org/10.1007/s11069-011-0080-6>
- Saroglou, H., Asteriou P., Zekkos, D., Tsiambaos, G., Clark, M., Manousakis, J. (2018). UAV-based mapping, back analysis and trajectory modeling of a coseismic rockfall in Lefkada island, Greece. *Natural Hazards and Earth System Sciences*. 18. 321-333. 10.5194/nhess-18-321-2018.
- Sokos, E., Zahradnik, J., Gallovič, F., Serpetsidaki, A., Plicka, V., Kiratzi, A. (2016). Asperity break after 12 years: The Mw6.4 2015 Lefkada (Greece) earthquake: The Mw 6.4 2015 Lefkada earthquake. *Geophysical Research Letters*. 43. 10.1002/2016GL069427.
- Spencer E. (1967). *A Method of Analysis of The Stability of Embankments Assuming Parallel Interslice Forces*. Geotechnique. 17: 11-26 TAGA Engineering Software Ltd (2019). TSLOPE technical information. Retrieved from <https://tagasoft.com/tslope-technical-information/>
- Terzaghi, K. (1950). *Mechanism of landslides*, Berkeley: Geological Society of America. pp. 83–123. <https://doi.org/10.1130/Berkey.1950.83>

- U.S. Department of Transportation Federal Highway Administration (2011). LRFD Seismic Analysis and Design of Transportation Geotechnical Features and Structural Foundations, Publication No. FHWA-NHI-11-032, GEC No3, Chapter 6, pp.6-10.
- Zekkos, D., Clark, M., Cowell, K., Medwedeff, W., Manousakis, J., Saroglou, H., Tsiambaos, G. (2017). Satellite and UAV-enabled mapping of landslides caused by the November 17th 2015 Mw 6.5 Lefkada earthquake, in: Proc. 19th Int. Conference on Soil Mechanics and Geotechnical Engineering, 17–22 September 2017, Seoul, 2017
- Zekkos, D, Greenwood, W., Lynch J., Manousakis, J., Zekkos, A., Clark, M., Cook, K. & Saroglou, H. (2018). Lessons Learned from The Application of UAV-Enabled Structure-From-Motion Photogrammetry in Geotechnical Engineering. 4. 254. 10.4417/IJGCH-04-04-03.